Title
Expression of the type VI intermediate filament proteins CP49 and filensin in the mouse lens epithelium.

Permalink
https://escholarship.org/uc/item/2q63c2vn

Authors
FitzGerald, Paul
Sun, Ning
Shibata, Brad
et al.

Publication Date
2016

Peer reviewed

Expression of the type VI intermediate filament proteins CP49 and filensin in the mouse lens epithelium

Paul FitzGerald, Ning Sun, Brad Shibata, John F. Hess

Department of Cell Biology and Human Anatomy, School of Medicine, University of California Davis, CA

Purpose: The differentiated lens fiber cell assembles a filamentous cytoskeletal structure referred to as the beaded filament (BF). The BF requires CP49 (*bfsp2*) and filensin (*bfsp1*) for assembly, both of which are highly divergent members of the large intermediate filament (IF) family of proteins. Thus far, these two proteins have been reported only in the differentiated lens fiber cell. For this reason, both proteins have been considered robust markers of fiber cell differentiation. We report here that both proteins are also expressed in the mouse lens epithelium, but only after 5 weeks of age.
Methods: Localization of CP49 was achieved with immunocytochemical probing of wild-type, CP49 knockout, filensin knockout, and vimentin knockout mice, in sections and in the explanted lens epithelium, at the light microscope and electron microscope levels. The relationship between CP49 and other cytoskeletal elements was probed using fluorescent phalloidin, as well as with antibodies to vimentin, GFAP, and α-tubulin. The relationship between CP49 and the aggresome was probed with antibodies to γ-tubulin, ubiquitin, and HDAC6.
Results: CP49 and filensin were expressed in the mouse lens epithelium, but only after 5 weeks of age. At the light microscope level, these two proteins colocalize to a large tubular structure, approximately 7 × 1 μm, which was typically present at one to two copies per cell. This structure is found in the anterior and anterolateral lens epithelium, including the zone where mitosis occurs. The structure becomes smaller and largely undetectable closer to the equator where the cell exits the cell cycle and commits to fiber cell differentiation. This structure bears some resemblance to the aggresome and is reactive with antibodies to HDAC6, a marker for the aggresome. However, the structure does not colocalize with antibodies to γ-tubulin or ubiquitin, also markers for the aggresome. The structure also colocalizes with actin but appears to largely exclude vimentin and α-tubulin. In the CP49 and filensin knockouts, this structure is absent, confirming the identity of CP49 and filensin in this structure, and suggesting a requirement for the physiologic coassembly of CP49 and filensin.
Conclusions: CP49 and filensin have been considered robust markers for mouse lens fiber cell differentiation. The data reported here, however, document both proteins in the mouse lens epithelium, but only after 5 weeks of age, when lens epithelial growth and mitotic activity have slowed. Because of this, CP49 and filensin must be considered markers of differentiation for both fiber cells and the lens epithelium in the mouse. In addition, to our knowledge, no other protein has been shown to emerge so late in the development of the mouse lens epithelium, suggesting that lens epithelial differentiation may continue well into post-natal life. If this structure is related to the aggresome, it is a rare, or perhaps unique example of a large, stable aggresome in wild-type tissue.

The first hint that lens fiber cells assembled an unusual cytoskeletal element emerged in the work of Maisel and Perry in 1972 [1]. These investigators used electron microscopy (EM) to document the presence of a "beaded chain filament" (now beaded filament, or BF). The BF was structurally distinct from thin filaments, intermediate filaments (IFs), and microtubules. Electron microscopy of "ghosted" fiber cells showed that BFs form a robust filamentous meshwork in elongated fiber cells of the outer lens cortex [2,3]. Antibodies suggested that two proteins, CP49 (aka phakosin, phakinin; gene name *bfsp2*) and filensin (aka CP115, CP95; gene name *bfsp1*) localized to this structure [4-7].

Using DNA sequencing, Remington was the first to draw the link between filensin and the IF family [8], a link solidified by subsequent sequencing efforts [9-12] and finally gene mapping [11,13-16]. However, the BF proteins stood out among the several score members of the IF family as the most divergent IF proteins yet identified. Both showed considerable sequence variation, including variations at some of the otherwise most highly conserved "signature" motifs of IF proteins. Notably, the BF proteins are not found in canonical 8–11 nm IFs. For these reasons, the BF proteins were designated as members of a new class in the IF family, the type VI orphan filaments [17,18].

Although BF proteins have been identified in at least five vertebrate orders [19], published reports have not documented the presence of BF proteins outside the lens fiber cell. Therefore, the BF proteins have been considered robust makers of fiber cell differentiation. Both proteins become

Correspondence to: Paul FitzGerald, Department of Cell Biology and Human Anatomy, School of Medicine, University of California Davis, Davis, CA 95616, Phone: (530) 752 7130, email: pgfitzgerald@ucdavis.edu

immunocytochemically detectable shortly after fiber cell elongation initiates and accumulate to high levels by the time elongation is completed. Surprisingly, germline knockouts of both BF proteins resulted in mice born with lenses that were optically clear to the naked eye [3,20,21]. With careful slit-lamp examination, a mild light scatter emerged at about P21, which grew progressively more pronounced with age. However, this light scatter never approached what would be described as an obvious cataract [3,20].

A much more pronounced change in the CP49/filensin knockout phenotypes was observed using scanning electron microscopy (SEM). This approach effectively conveys the extraordinary structural differentiation undergone by the lens epithelial cell as it matures into a fiber cell, as well as the striking degree of long-range order with which fiber cells assemble into a tissue. This remarkable structural differentiation and organization are hallmarks of all vertebrate lenses, and therefore have been considered essential to optical clarity. In BF knockout mice, the initial phases of fiber cell elongation and stacking proceed normally. However, deeper in the cortex the fiber cells undergo a near-total loss of this highly ordered architecture. Despite this loss of the structural phenotype, the knockout (KO) lenses exhibit only a minor loss of optical clarity [4]. This disproved the long-held assumption that the exquisite structural order that characterizes vertebrate lenses was essential for optical transparency. More detailed examination of the KO lenses has shown that in addition to an essential role in maintaining the fiber cell and lens structural phenotype, the BFs also contribute to optical fidelity [21], lens shape, and lens mechanical properties [22].

The knockout animals further established that both CP49 and filensin were required for BF assembly, suggesting obligatory coassembly [3,20,23]. Genetic elimination of either CP49 or filensin resulted in a sharp reduction in the "unmated" assembly partner [3,20,21]. This mutual interdependence for stability may represent a mechanism that regulates stoichiometry, but it likely also protects the cells against protein aggregation toxicity: Similar to their IF brethren, BF proteins are not soluble under physiologic conditions, and in the absence of an assembly partner the unmated protein is likely recognized as an unfolded protein and removed. This closely mimics data that have been reported for epidermal keratins, which also form obligate heterodimers [24].

In this report, we document the robust expression of both BF proteins in the mouse lens epithelium. This epithelial expression does not become detectable until 5 weeks of age, and then only in the anterior and anterolateral epithelium. Light microscopy localizes both BF proteins to a discreet, compact, vermiform ("worm-shaped") structure, which is not delimited by a lipid bilayer. This structure appears to be the same as that described by Nancy Rafferty as a "sequestered actin bundle," a term that was coined before the elucidation of the BF story [25]. In the present study, the relationship of this structure to established organelles and cytoskeletal systems is explored, as is the relationship to the aggresome, a structure in which unfolded proteins are sequestered for subsequent removal by autophagic mechanisms.

METHODS

Antibody sources: Affinity-purified rabbit polyclonal antibodies were raised to chromatographically-purified, recombinant CP49, filensin, and vimentin, and characterized as described in previous reports [3,20]. Chicken antibodies to CP49, generated from chromatographically-purified, recombinant mouse CP49 were custom made by Aves laboratories (Tigard, OR). Rabbit antibody to γ-tubulin was a gift from Ken Beck (University of California [UC] at Davis). Antibody to HDAC6 [26] was generously provided by Tso-Pang Yao (Duke University). Antibody to α-tubulin was purchased from Sigma-Aldrich (Cat No. T-6199; St Louis, MO). Alexa Fluor 488 and 555 goat anti-rabbit and goat anti-chicken antibodies were purchased from Life Sciences Technology (Waltham, MA). Rabbit anti-GFAP was purchased from Epitomics (Cat. No. 2301–1; Burlingame, CA). Goat anti-rabbit 10 nm colloidal gold was purchased from BBI Solutions (Madison, WI). Alexa Fluor–labeled phalloidin (Invitrogen, Waltham, MA) was used at 1:20 dilution. Mouse monoclonal anti-ubiquitin antibody (VU-1) was purchased from LifeSensors (Cat. No. VU101; Malvern, PA). Mouse monoclonal antibody to ubiquitin (clone Ubi-1/042691GS) was purchased from Millipore (Cat. No. MAB1510; Danvers, MA).

Light microscope–level Immunocytochemistry: For labeling sectioned material, unless otherwise noted, the mouse eyes were fixed with freeze substitution as described by Sun et al. [27] and subsequently embedded in paraffin. Briefly, eyes were removed and plunged into −80 °C propane for 1 min, transferred to −80 °C methanol:acetic acid (97:3), and stored at −80 °C for 48 h. Vials were moved to −40 °C, −20 °C, and room temperature for 2 h each. Methanol-acetic acid was then exchanged for 100% ethanol. Eyes were embedded in paraffin using routine dehydration and infiltration routines. Four-micron sections were deparaffinized through xylene and ethanol, and rehydrated into PBS (100 mM NaPhosphate, 154 mM NaCl, pH 7.4). Sections were blocked for 15 min with normal goat serum in Tris-buffered saline, 0.1% Tween-20 (TBST). Incubation with antibodies was conducted 4 h to overnight in blocker, and washed 3X for 10 min each in TBST and then into secondary antibodies for

4 h. All diluted antibody solutions were spun at 14,000 ×g for 10 min before use. Controls consisted of substitution of non-immune primary antibody for a specific antibody. The specific antibodies used for labeling ubiquitin did not work in freeze-substituted tissue; therefore, fixation was achieved by immersion in 4% paraformaldehyde in PBS. Because both anti-ubiquitin antibodies were mouse IgG1 monoclonal antibodies, and this was mouse tissue, the controls consisted of an irrelevant mouse IgG1 monoclonal antibody substituted for the primary anti-ubiquitin antibody.

For electron microscope–level immunocytochemistry, lenses were fixed in 3.5% formaldehyde in PBS for 5 h and then immersed in PBS for 48 h. Lenses were stained en bloc with 1% uranyl acetate (UA) and then dehydrated in 100% ethanol. A patch of the anterior lens was dissected free of the underlying fiber cell mass and equilibrated in 100% LR White (Cat No. 14383, EMS, Hatfield, PA) for 48 h. Polymerization of LR White was achieved with ultraviolet (UV) light, under nitrogen, at room temperature. Silver-gold sections were harvested onto carbon formvar grids, blocked with normal goat serum (NGS), and probed with primary antibodies for 2 h. Grids were washed in TBST and then labeled with 10 nm gold conjugated to goat anti-rabbit antibodies for 2 h. After washing as above, the grids were fixed again with glutaraldehyde, given a final wash in deionized water, and stained with UA. Lens "ghosts" were prepared as described [2]. Briefly, freshly isolated lenses were frozen in optimum cutting temperature (OCT), and 150 μm sections harvested at −14 °C in a cryostat. Sections were floated on ice-cold TBS to allow crystallins to diffuse away, then fixed with glutaraldehyde and formaldehyde, and embedded in Poly/ Bed 812 (Polysciences, Warrington, PA) for thin sectioning using routine methods. Isolated filaments were prepared by first gently disrupting the decapsulated lens cortex in ice-cold TBS, using a stirring flea for 10 min. The disrupted cortex was homogenized using a Dounce homogenizer and then pelleted at 50,000 ×g av for 30 min to separate soluble crystallins from insoluble membrane-cytoskeleton complex. The pellet was rinsed with TBS and homogenized again, and a 10 μl droplet was placed on a glow discharged, carbon-formvar-coated 300 mesh copper grid (Pelco, Redding, CA) and negatively stained with 1% aqueous uranyl acetate.

Explants were prepared by placing a lens anterior side down on dry filter paper and then opening the capsule with fine forceps at the posterior pole. Flaps of the capsule were pressed to the filter paper at three points, and the lens was gently lifted off the adhering capsule and epithelium complex. The explant was then flooded with 4% formaldehyde in PBS for 5 min to stabilize it. Explants were then removed to a stainless steel basket (to facilitate handling) in a 24-well tissue culture plate for another 15 min of fixation. Explants were rinsed with PBS containing 50 mM glycine to block aldehydes, and 0.5% Triton X-100 to permeabilize the cells, then rinsed with PBS, and finally and blocked with TBST-NGS for immunolabeling. Primary antibody was left on overnight, at 4 °C, then washed 3X at 15 min each, at room temperature. Secondary antibody was added and incubated at room temperature for 4 h. Explants were placed on a microscope slide and examined with either a Nikon Eclipse E800 epifluorescent microscope (Nikon, Melville, NY), an Olympus FV1000 confocal microscope (Center Valley, PA), or a Leica SP8 TCS STED 3X, configured for super resolution imaging (Buffalo Grove, IL).

Knockout mice: CP49 and filensin knockouts were generated and then outbred to congenicity with C57BL/6 mice as described [3,20]. Vimentin knockout mice were originally created by Colucci-Guyon, rederived at UC Davis, and then similarly outbred [28]. Because some mice strains, including those most commonly used for KO and transgenic generation, bear a large deletion in the CP49 locus that results in a de facto CP49 knockout [23,29,30], all mice were tested to ensure the presence of the wild-type (WT) allele.

Image processing: Digitally-captured images were subjected to processing using Photoshop (Adobe Systems, San Jose, CA). Image levels were adjusted so that the exposure range spanned from white to black to maximize the gradation of intensity. For images captured from explants, where considerable Z-axis variation occurred due to folding and curling induced by the capsule, local expansion of contrast was used to balance the image intensity across the image to fall within the usable range. Super-resolution images were subjected to deconvolution using Huygens Professional and Bitplane Imaris software. All mice procedures were approved by the UC Davis Institutional Animal Care and Use Committee and were in compliance with the ARVO policy statement on the use of animals in research.

RESULTS

Beaded filament proteins in the mouse lens epithelium: Figure 1A presents an overview of the CP49 immunolabeling in the anterior and anterolateral lens epithelium in the paraffin section. The lens is oriented with the anterior pole at the 12 o'clock position. As expected, CP49 reactivity (CP49 = green channel; 4',6-diamidino-2-phenylindole [DAPI]-labeled nuclei = blue channel) is abundant in the fiber cells. However, this image also shows discreet CP49 labeling in the lens epithelium (white arrows, Figure 1A). Arrows in Figure 1A identify three examples of a well-defined structure that is

reactive with CP49 antibodies, but more than 30 are present in this image. More detail is revealed in a higher magnification view of sectioned material, shown in Figure 1B. A more informative view of this structure is seen in Figure 2A, an en face view of an immunolabeled mouse lens epithelial explant. The CP49-reactive structure is typically found in a perinuclear location, usually, although not always, at a frequency of one per cell. Although the sections show a mix of tubular and circular structures, Figure 2 makes it clear that the structure is typically tubular, suggesting that the circular profiles seen in sections result from orientation or plane-of-section. This structure has a well-conserved and clearly defined "vermiform" or worm-like shape (i.e., generally tubular with tapered ends). Although the structure remains cylindrical in the cross section, there is some pleomorphism in the overall shape, as can be seen in Figure 2B–F. These examples all retain a tube-like configuration, but the tube is contorted into various shapes. Figure 2F includes a scale bar of 10 µm to provide a perspective on the dimensions. The example in Figure 2F is approximately 7 µm long x 1 µm in diameter.

To determine whether these structures were reactive for CP49 and filensin, explants were double-labeled with chicken antibodies to CP49 (Figure 2G) and rabbit antibodies to filensin (Figure 2H) and then imaged with stimulated emission depletion (STED) super-resolution microscopy. The merged image is shown in Figure 2I. Although both proteins were always present, some subtle degree of non-coincident labeling could be seen in the 0.1 µm optical sections (not shown) or after the deconvolution of the STED super-resolution images was pushed (Figure 2J). The non-coincident labeling was somewhat variable. However, because both proteins were always present, subsequent results are presented only for CP49.

Figure 3A is oriented with the lens anterior pole at the 12 o'clock position. This image demonstrates that the epithelial CP49 reactivity (the green channel) is most robust in the anterior and anterolateral epithelium but begins to diminish in the region just anterior to the bow, becoming smaller, and less frequent nearer the lens coronal equator, until the reactivity
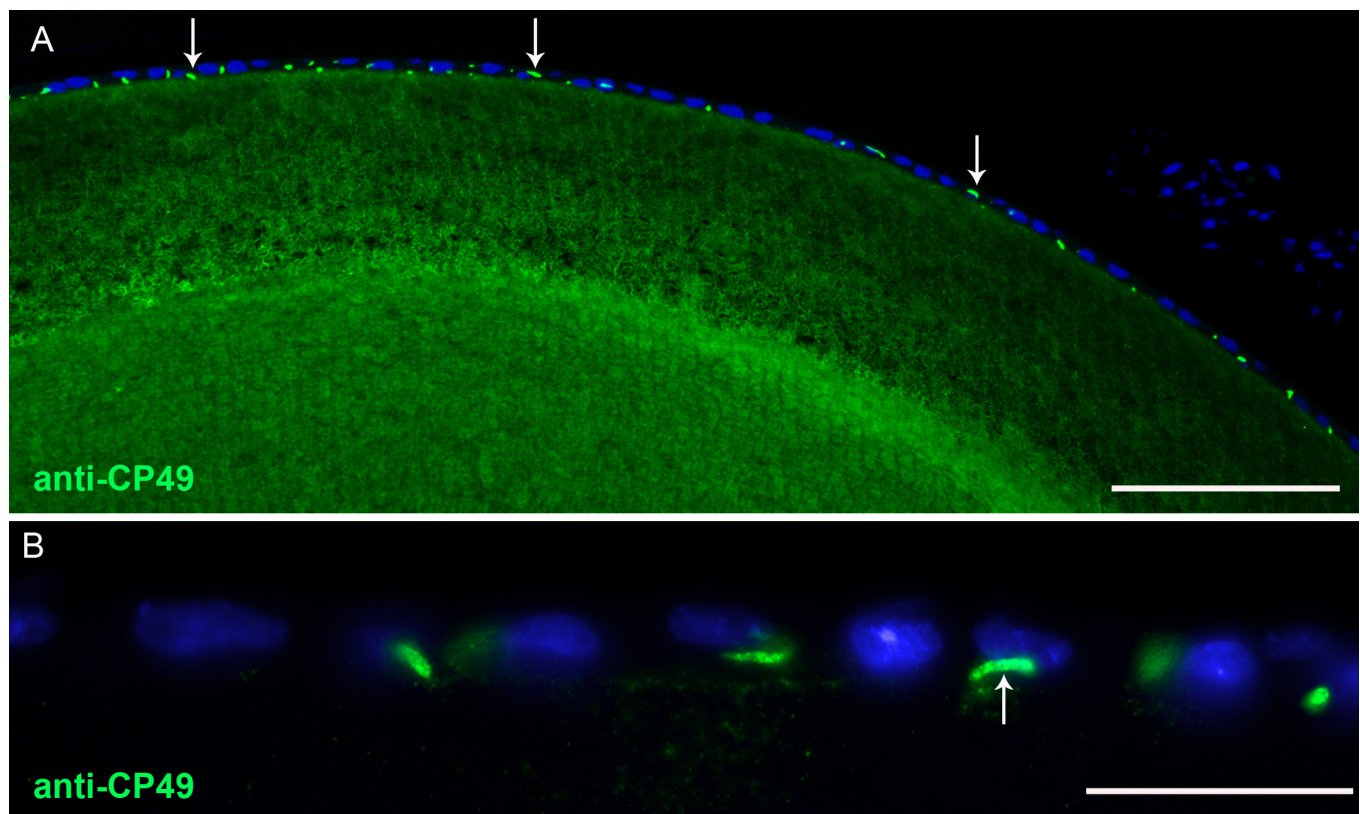

Figure 1. BF proteins are found in the mouse lens epithelium. **A**: Sagittal paraffin section of mouse lens labeled with antibodies to CP49 (green channel) and 4',6-diamidino-2-phenylindole (DAPI; blue channel). The image is oriented so that the anterior pole is at the 12 o'clock position. White arrows identify three of more than 20 examples of the CP49-reactive structure in the lens epithelium (scale bar = 100 µm). **B**: Higher magnification view of the lens epithelium labeled as in **A**, with a good example of this CP49 reactive structure highlighted by the white arrow (bar = 20 µm).
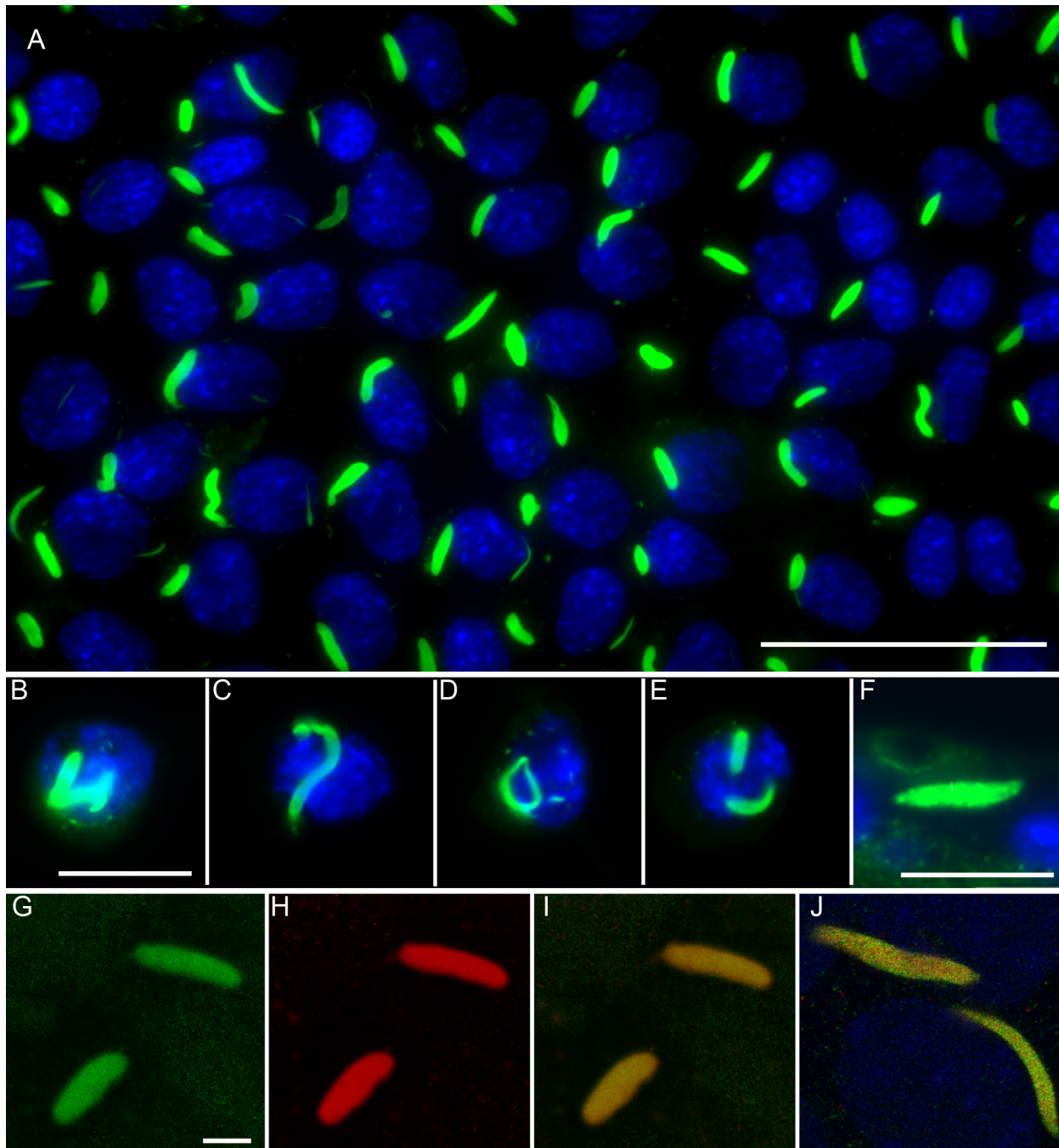
Figure 2. En face view of the lens epithelium. **A**: A lens capsule/epithelial explant labeled for CP49 (green channel) and 4',6-diamidino-2-phenylindole (DAPI; blue channel), showing the relative uniformity of the size and distribution of this structure in the anterior epithelium (scale bar = 30 µm). **B–F**: Although the beaded filament (BF)-positive structure is predominantly tubular, its overall shape can vary (CP49 = green channel). **E**: This structure can be present at two copies per cell (**B–E** scale bar = 10 µm). **F**: High magnification view of a fully elongated example (scale bar = 10 µm). **G–H**: Stimulated emission depletion (STED) super-resolution imaging of a lens epithelial explant labeled for CP49 (**G**, green), filensin (**H**, red), and merged (**I**). **J**: Deconvoluted image of colocalized CP49 and filensin showing that there may be some degree of substructure, or non-coincident labeling of CP49 and filensin (**G–H** scale bar = 2 µm).

is largely undetectable. A higher magnification view of the region just anterior to the equator is shown in Figure 3B that is colocalized with EdU, a marker for recently divided cells (red channel). This shows that the CP49-reactive structure begins this processing or dismantling in the region where the epithelial cells are mitotically active. Figure 3C shows the remnants of the CP49-reactive structure (white arrows) near the coronal equator. CP49 immunoreactivity then reemerged in the elongating fiber cells as has been described.

Anti-CP49 labeling of the epithelium in the CP49 knockout lens was negative. Similarly, anti-filensin labeling of the filensin knockout lenses was negative (negative results not shown). These results confirm the identity of the proteins labeled with these antibodies.

EM-level Immunocytochemistry and Structure: To gain further insight, we extended the anti-CP49 localization to the electron microscope level (Figure 4). Figure 4A shows a lower magnification overview of three lens epithelial cells ("N" identifies nuclei; the white arrow identifies the lens capsule). The black arrows identify the CP49-reactive structure. At higher magnification (Figure 4B), the CP49 reactivity is evidenced by the abundant gold labeling. This structure presents as a dense accumulation of protein, lacking a limiting lipid bilayer, and commonly showing small, round, electron-lucent sites (black arrow). The structure was "fuzzy" in texture, with some suggestion of filamentous composition. Filamentous cytoskeleton can be seen peripheral to this structure (white arrow).

Because tissue processed for EM immunocytochemistry usually represents a tradeoff between structural preservation and immunogenicity, the structure was subsequently reimaged using conventional epoxy resin/heavy metal–stained samples (Figure 4C). However, this revealed no additional detail or substructure. To directly compare the structure of the BF-positive structure in the lens epithelium to what has been described in the fiber cells, we prepared "ghosts" of the lens epithelium (Figure 4D) and fiber cells (Figure 4E). Figure 4E shows part of a single fiber cell from the superficial cortex. Canonical IFs can be seen surrounding the black asterisk, and fiber cell BFs can be seen surrounding the white asterisk. The fine structure of the BF can be seen in the inset (Figure 4F) of the BFs isolated from the homogenized lens and imaged with negative staining. This reveals an approximately 3 nm core filament decorated by 12–15 nm beads at 20 nm intervals. In the lens epithelium (Figure 4D), canonical IFs can be seen at the black asterisk, while the CP49-reactive structure can be seen at the white asterisk. If the BF proteins of the epithelium are assembled into BFs, it cannot be determined from these images, possibly a result of compaction.

Codependence on CP49 and filensin: CP49 and filensin knockout mice have shown that both CP49 and filensin are required for BF assembly in fiber cells [3,20,21]. When either protein is eliminated by germline knockout, BFs do not assemble, and the "unmated" assembly partner is mostly removed. To ask whether this lens epithelial structure was also dependent on coassembly of CP49 and filensin, we labeled the CP49 knockout lenses with antibodies to filensin and the filensin knockout lenses with antibodies to CP49. We reasoned that if this epithelial immunoreactivity represented accumulated, misfolded aggregates of either or both proteins, then these proteins would behave independently: If one were absent, the other would still remain as an aggregate. Conversely, if they coassembled into a physiologic and stable heteromer, then the loss of one protein would result in the loss of the other, emulating what has been observed in the fiber cells of the knockout animals. Each localization was negative (not shown). No labeling of this structure was seen in either knockout. These data are consistent with the hypothesis that this BF protein-reactive structure in the lens epithelium represents a coassembly of the two BF proteins and that in the absence of an assembly partner, the unmated BF protein is removed.

Age-dependence in the appearance of BF proteins in the lens epithelium: To document the age-dependent appearance of CP49 in the lens epithelium, we conducted immunocytochemistry on paraffin sections of mouse eyes that ranged in age from 23 days to 1 year. Figure 5 shows labeling of CP49 in P28 (Figure 5A), P37 (Figure 5B,C), and P45 mice (Figure 5D). The P28 mouse (Figure 5A), while showing strong labeling of fiber cells (green channel), shows no indication of immunoreactivity in the epithelium (compare to Figure 5D). At 37 days (Figure 5B), however, the first evidence of these structures begins to appear. Although they are too small to be readily seen at the magnification used in Figure 5B, a higher magnification view of the 37 day lens epithelium shown in Figure 5C reveals the first appearance of these structures (highlighted by white arrows). Eight days later, the structure is present in essentially all anterior and anterolateral epithelial cells (Figure 5D, P45 lens). Labeling of 1-year-old mice established that this structure remains a feature of the lens epithelium until at least 1 year (not shown). These data show that the emergence of the CP49 reactivity occurs during a short window of time starting at about 5 weeks of age and is a feature of the lens epithelium for at least 1 year.

Relationship to other cytoskeletal elements: Electron microscopy showed this structure is in close proximity to other filamentous cytoskeletal elements (white arrow, Figure 5B).
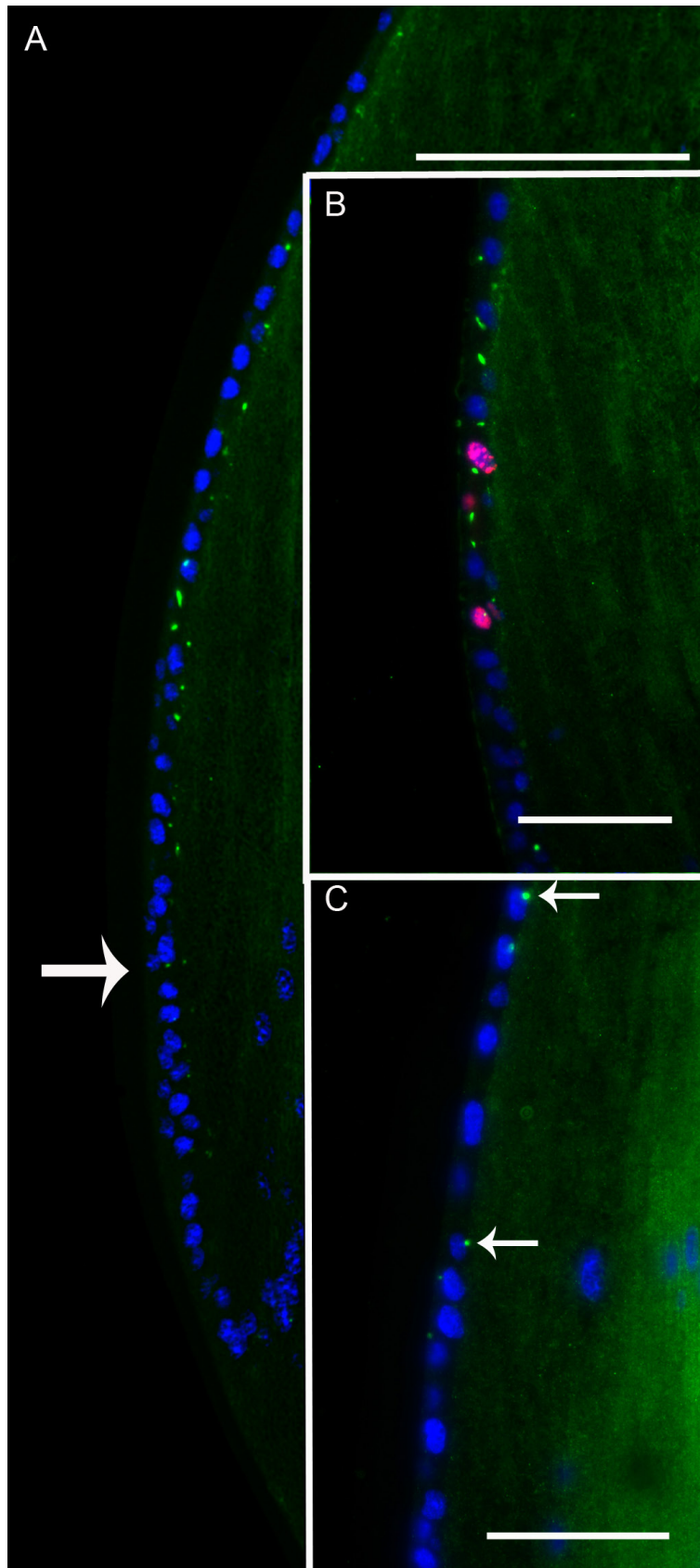
Figure 3. Spatial distribution of epithelial labeling. **A**: Paraffin section overview of the anterior lens labeled for CP49 (green channel) and oriented with the anterior pole at the 12 o'clock position. The CP49-reactive epithelial structure becomes smaller and punctate, and then finally disappears near the coronal equator. The last obvious indication of CP49 reactivity in epithelial cells occurs at about the white arrow (scale bar = 200 μm). **B**: Colocalization of EdU (red channel) that labels recently divided cells and the CP49-reactive structure. It is evident that the loss of the vermiform shape occurs in the region of the lens where the epithelium is mitotically active (scale bar = 150 μm). **C**: At higher magnification, arrows identify one of the punctate remnants. Deeper in the lens cortex, CP49 reactivity once again begins to accumulate in the maturing fiber cells (**C**, right-hand edge) as has been reported previously. Scale bar = 100 μm.
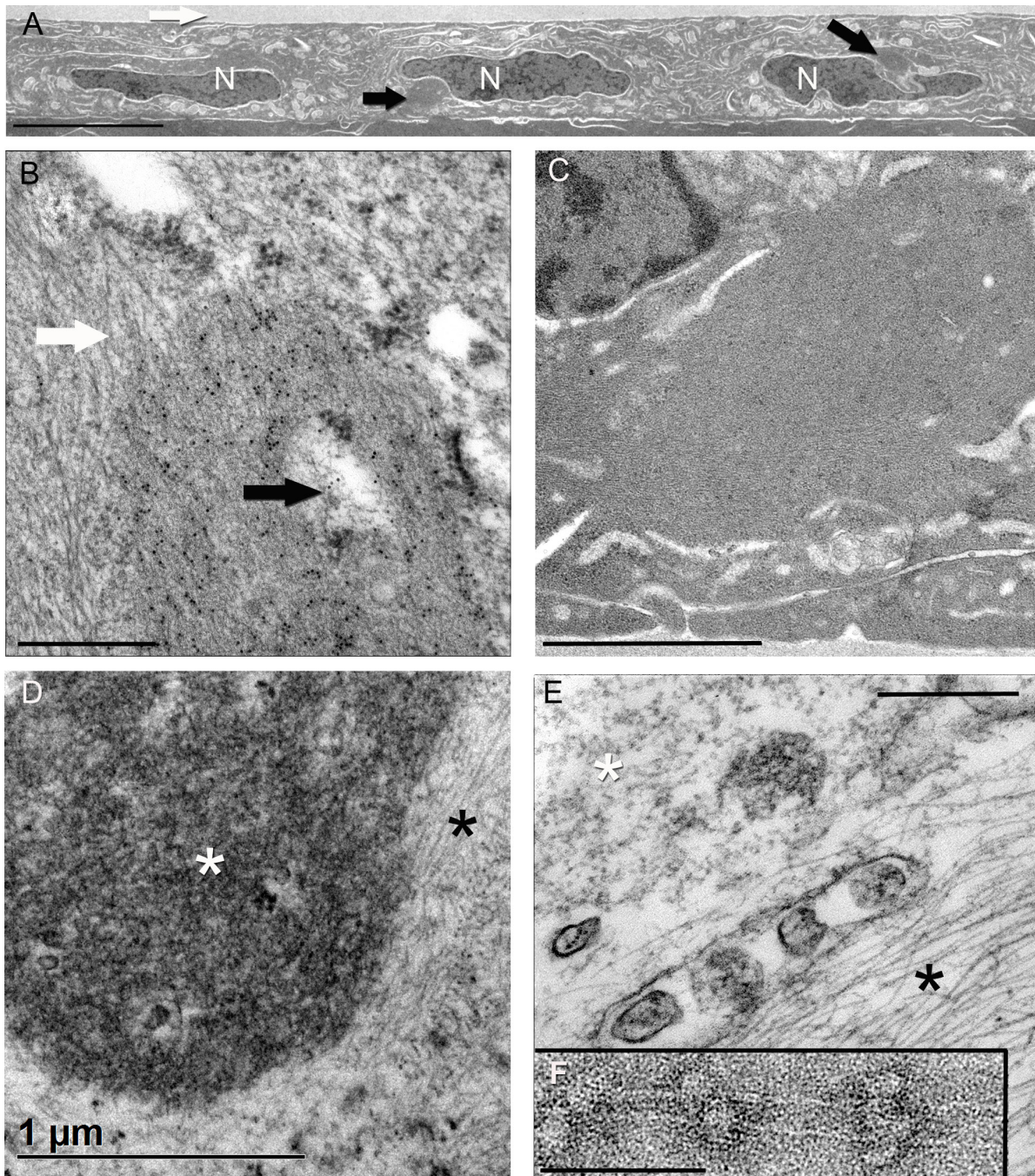
Figure 4. Electron microscopy. **A**: An overview of parts of three mouse lens epithelial cells ("N" = nucleus). The capsule is indicated by the white arrow at top and the CP49-reactive structures by the black arrows (scale bar = 8 µm). **B**: Higher magnification view of the vermiform structure shows CP49 immunoreactivity, revealed by the presence of 10 nm gold particles. This structure commonly exhibits an electron lucent region (example, black arrow). The structure is surrounded by a meshwork of filaments (white arrow). Scale bar = 1 µm. **C**: Routine transmission electron microscopy (TEM) of the lens epithelial cell (scale bar = 1 µm). The structure is dense enough that any substructure is not obvious under routine immersion-fixation conditions. **D–E**: The "ghosted" lens epithelium (**D**) and fiber cell (**E**) display the beaded filaments (BFs) more readily when soluble proteins are allowed to diffuse away. **E**: A single fiber cell that exhibits BFs (white asterisk) and canonical intermediate filaments (IFs; black asterisk) highlighting the difference between these two classes of IFs. **F**: An isolated pair of BFs imaged with negative stain TEM, clearly revealing the BF structure (scale bar = 20 nm). The vermiform structure of the epithelium (white asterisk, **D**) does not clearly reveal obvious BFs, possibly due to compaction, or to assembly into some other format.
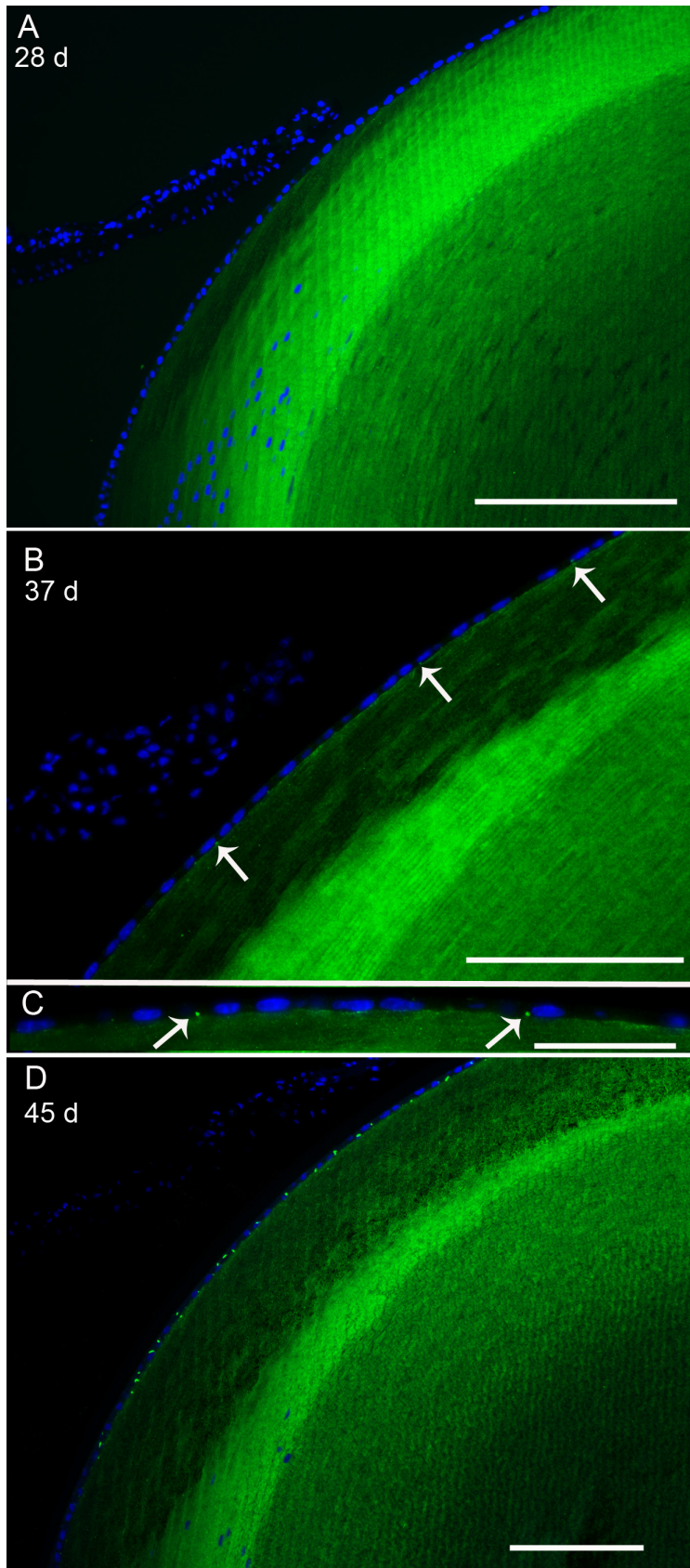
Figure 5. Temporal emergence epithelial CP49 reactivity. **A–D**: Labeling for CP49 (green channel) in lenses of different ages. **A**: 28-day mouse lens. No CP49 immunoreactivity is evident in the lens epithelium. Scale bar = 100 µm. **B**: 37-day mouse lens. Immunoreactivity is demarcated by the white arrows and shown at higher magnification in **C**. (**B**, scale bar = 50 µm; **C**, scale bar = 40 µm). **D**: Labeling of 45-day mouse lens shows robust CP49 reactivity in the lens epithelium (scale bar = 100 µm).
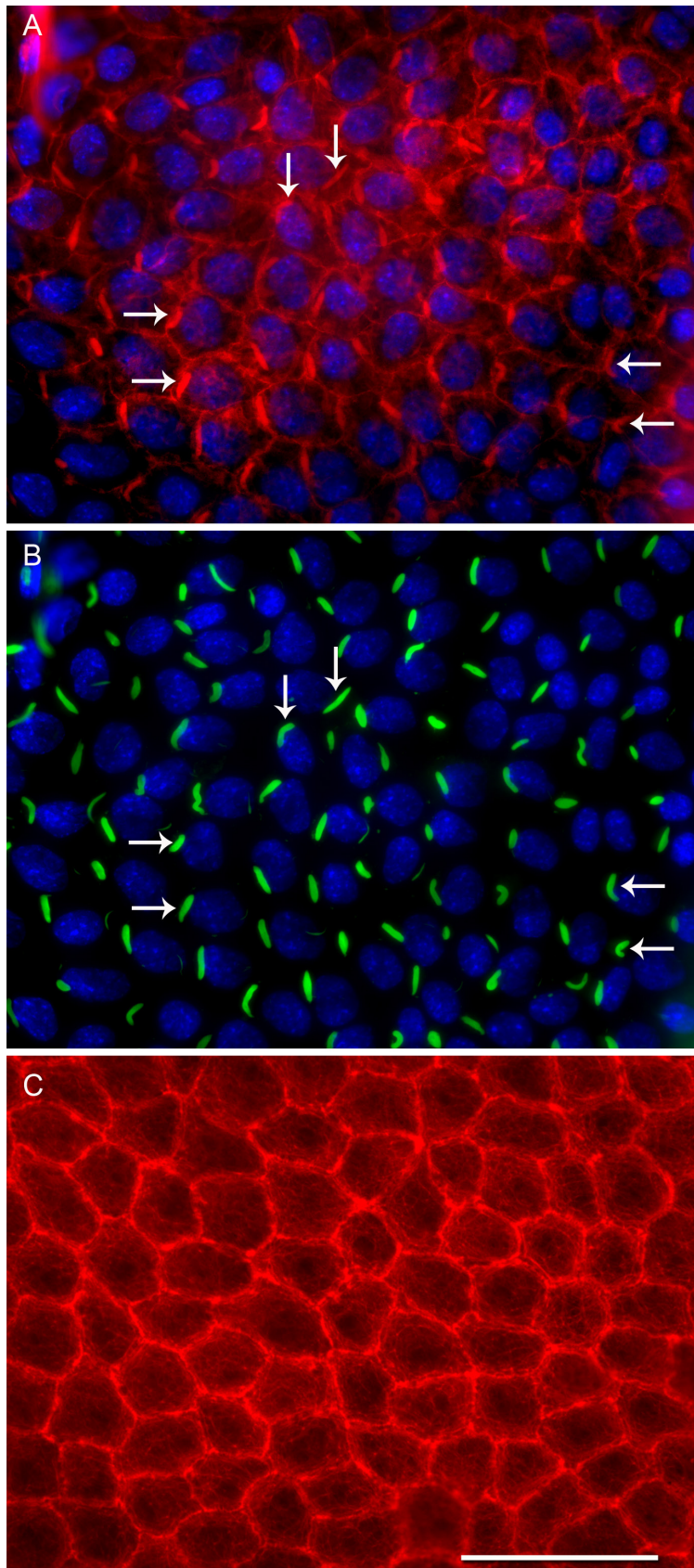
Figure 6. Actin and CP49 colocalize in the vermiform structure. **A**: Mouse lens epithelial explant labeled with phalloidin identifies filamentous actin (red channel). Arrows identify six examples (of several dozen) of the vermiform structure. **B**: The same field of view as in **A**, but captured in the green channel, which identifies labeling for CP49. The same six examples of the vermiform structure are demarcated with arrows. **C**: Phalloidin labeling of a lens epithelial explant from a CP49 knockout mouse shows a rich network of actin filaments (red channel) but no evidence of the vermiform structure (scale bar = 40 μm).
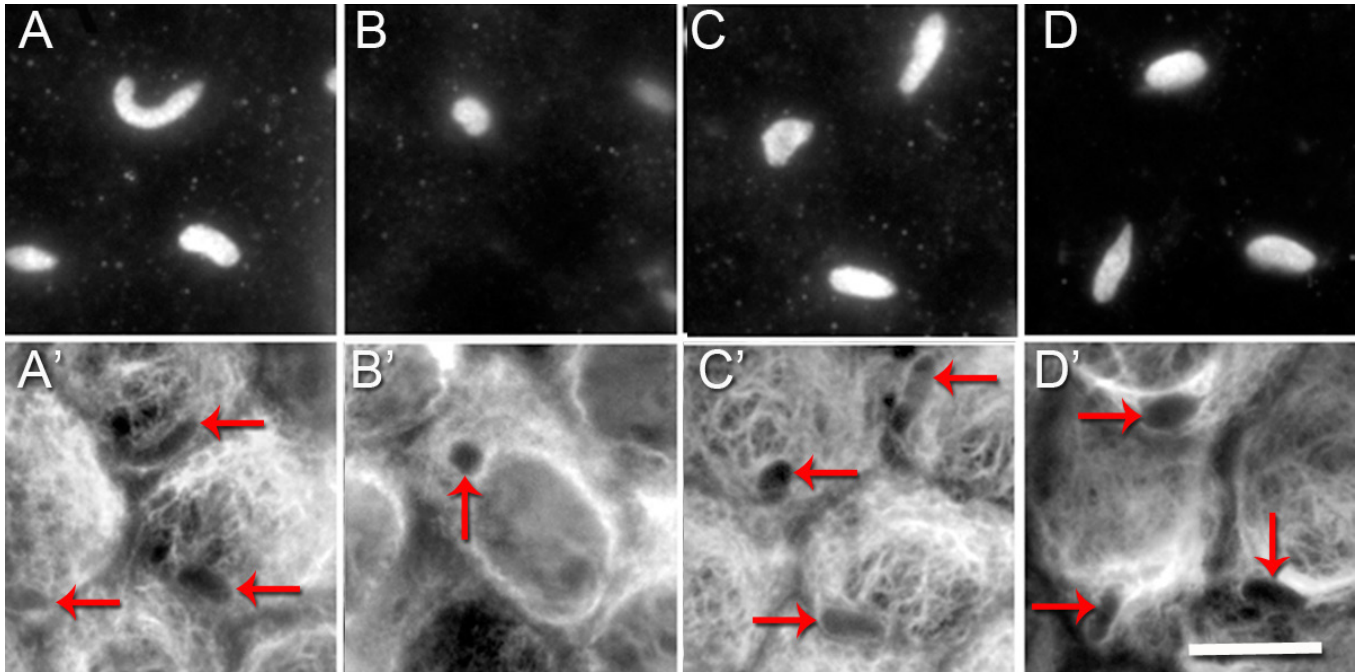
Figure 7. Colocalization of vimentin and CP49. A montage of four pairs of images taken from a lens epithelial explant double-labeled with antibodies to CP49 (**A–D**), and vimentin (**A'–D'**). The vermiform structure is clearly labeled with antibodies to CP49 in the upper panel, while the lower panel shows that vimentin is absent (or at much lower levels) in those same structures (marked by red arrows; scale bar = 10 μm).

To explore this, we colocalized CP49 with actin, vimentin, GFAP, and tubulin.

Figure 6A,B show the results of double labeling of a lens epithelial explant with phalloidin-Alexa Fluor 555, a probe for filamentous actin (red channel), and CP49 (green channel). Actin labeling occurs throughout the cell, in the cytoplasm and in the sub-membranous region as expected (Figure 6A), but phalloidin also intensely labels the CP49-reactive structure (white arrows). The colocalization of CP49 and actin in the vermiform structure is confirmed in Figure 6B which displays the green channel highlighting CP49 localization in the same field. Arrows highlight examples of coincident labeling of this structure for actin and CP49. CP49 does not show obvious colocalization with any other actin network in the epithelial cell.

To explore whether there was any evidence that this structure required both the BF and actin to assemble, we repeated the phalloidin labeling on explants of CP49 knockout mice. The results, presented in Figure 6C, show the expected cytoplasmic and sub-membranous presence of actin filaments in the epithelium but show no indication of the vermiform structure. These data indicate that actin alone is insufficient for this structure to form and that BF proteins are essential to its assembly.

Vimentin is by far the dominant IF protein in the lens epithelium. Double labeling with antibodies to CP49 and vimentin produced a complementary result to what was seen for actin labeling: Vimentin appears to be largely excluded from this structure. Figure 7 shows a montage of four paired images taken from explants double-labeled with antibodies to CP49 (Figure 7A–D) captured in the green channel and vimentin (Figure 7A'–D') captured in the red channel. Images are presented in black and white to better highlight the absence of staining. Images shown in Figure 7A'–D' establish that the cytoplasm of lens epithelial cells is rich in vimentin, but that numerous examples can be seen where there is an unlabeled region (red arrows) that exactly maps to the location of the CP49-reactive structure in the paired images in Figure 7A–D.

GFAP, also a type III IF protein, has also been documented in the lens epithelium of at least some strains of mice [31,32]. To explore the relationship between GFAP and the vermiform structure, we probed for the presence of GFAP. As an internal control to verify that the antibody reacted with mouse GFAP, we included the optic nerve in the section. In Figure 8A–B, labeling of the optic nerve head and anterior lens epithelium with rabbit anti-GFAP is compared. Figure 8B, captured at 80 ms exposure, shows intense labeling of the optic nerve head as expected, validating the antibody
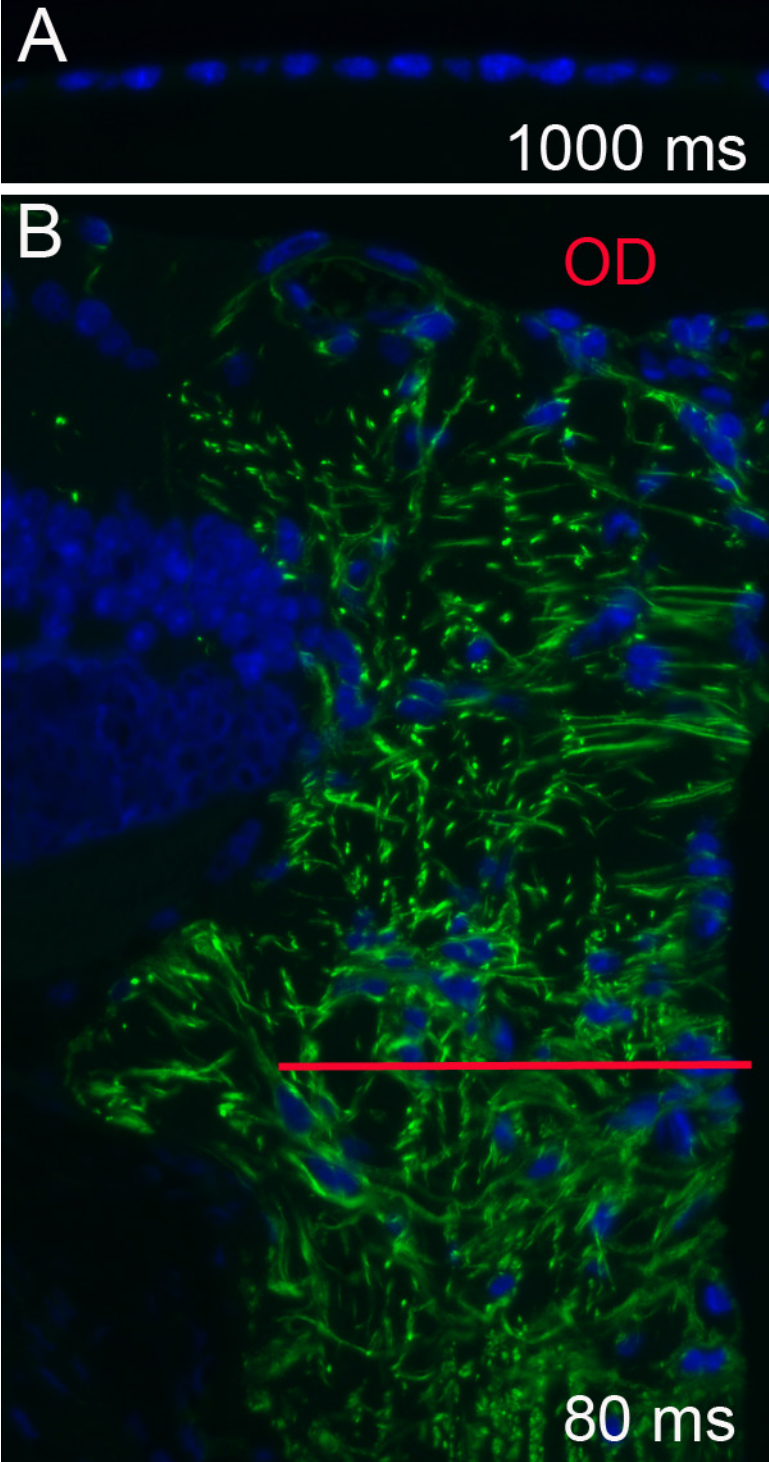
Figure 8. Localization of GFAP. Mouse whole eye section that includes the lens epithelium (**A**) and the optic disc region (in **B**). Rabbit antibodies to GFAP show intense labeling of the optic nerve (red bar region, **B**) exposed for 80 ms, but no reactivity in the anterior lens epithelium exposed for 1,000 ms (**A**). OD, optic disc.
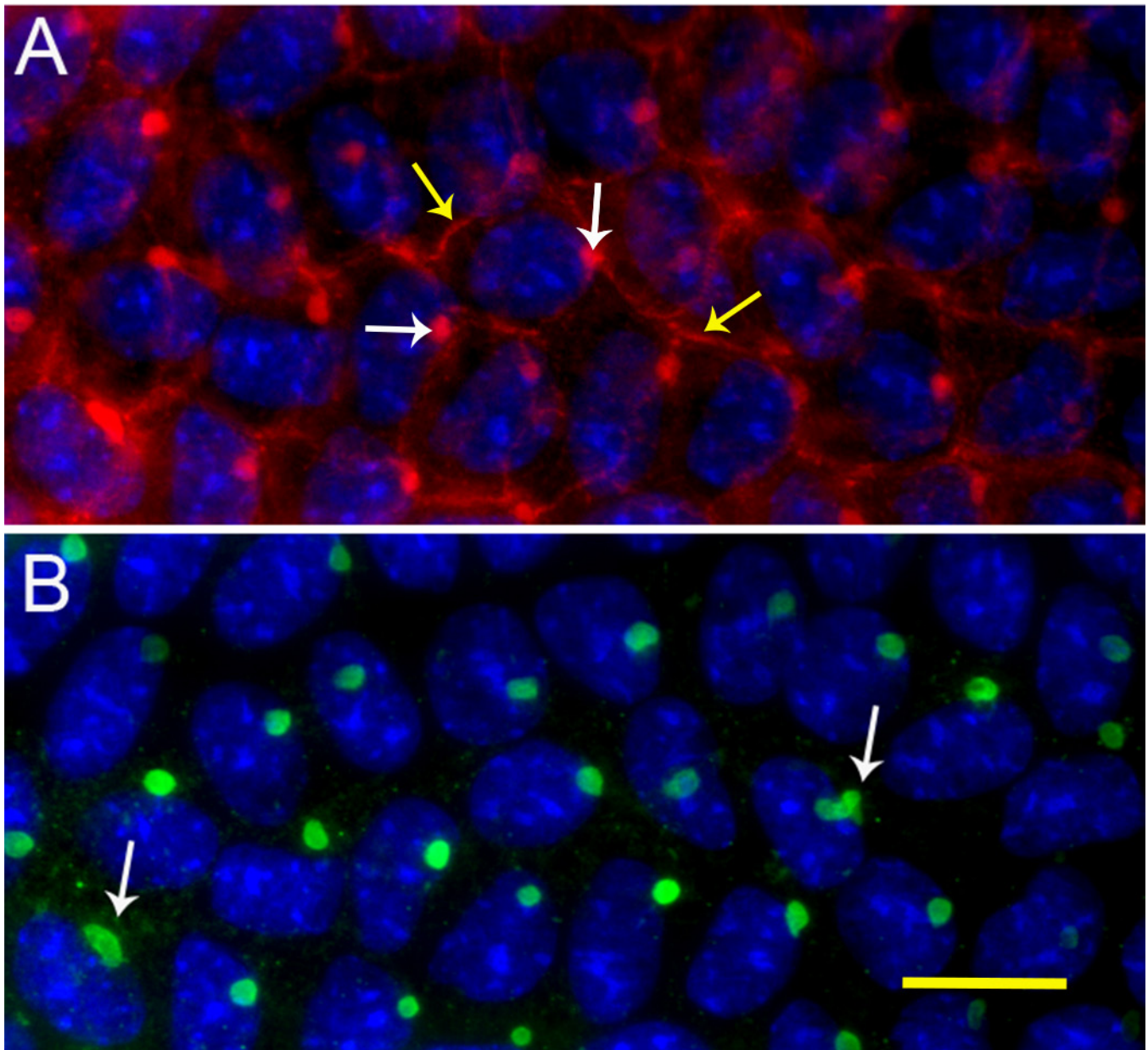
Figure 9. Localization of actin and CP49 in the vimentin knockout mouse. **A**: Phalloidin-labeled filamentous actin (red channel) in an explant of lens epithelium, showing the cortical actin network (yellow arrows), and the vermiform structure (white arrows). **B**: CP49 labeling of vermiform structure in an explant of the vimentin knockout mouse. Compared to Figure 2, it is evident that the absence of vimentin dramatically alters the shape of the vermiform structure. Labeling the vimentin knockout reveals that the structure changes from vermiform to predominantly round. Some exceptions are usually seen, as indicated by the white arrow in **B** (scale bar = 10 μm).

reactivity. Imaging of the lens epithelium in the same section, captured at 1,000 ms, did not reveal detectable GFAP reactivity. This suggests that GFAP is either absent or present at low levels in the lens epithelium of these mice and that GFAP is likely not required for the assembly of this structure.

To determine the degree to which vimentin influences the presence or properties of this structure, actin and CP49 were localized in explants from the vimentin knockout mouse. Figure 9 shows double labeling for actin (Figure 9A, red channel) and CP49 (Figure 9B, green channel) in the vimentin knockout mouse. The CP49-reactive structure is present, and it contains actin and CP49. However, the shape of most of these structures is round and not elongated. Some exceptions occur, as highlighted by the arrows. Figure 4B
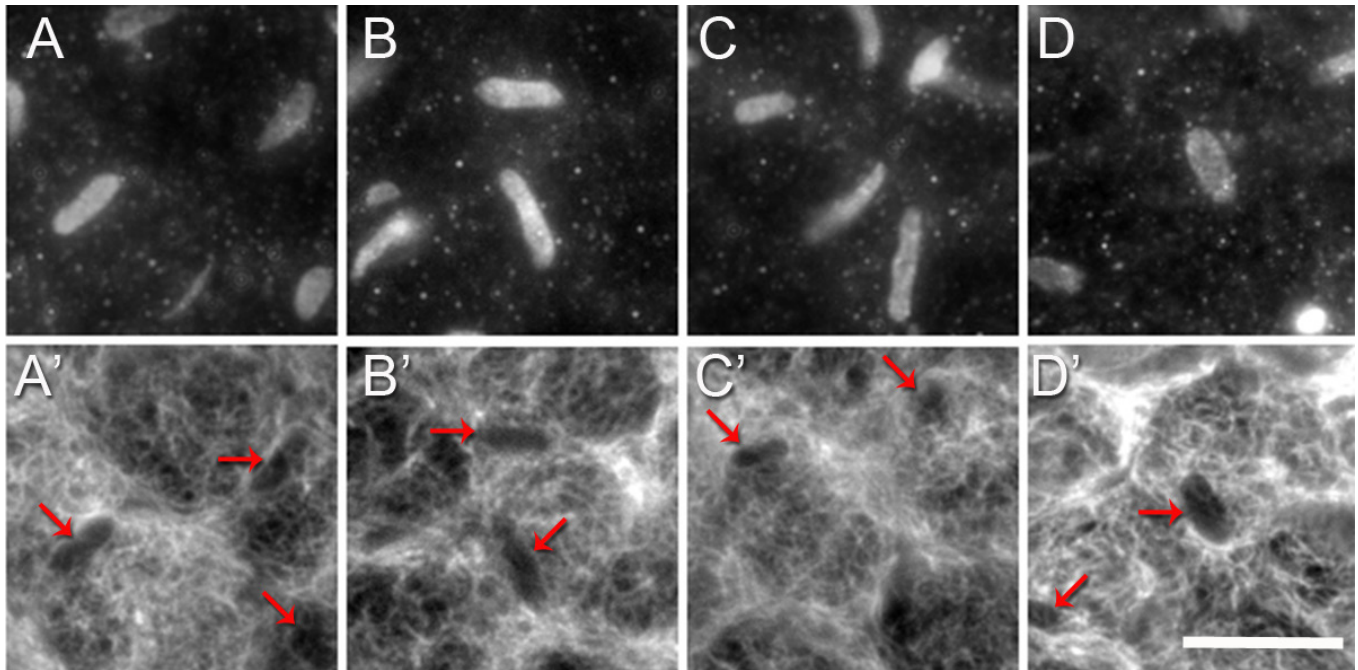
Figure 10. Colocalization of α-tubulin and CP49. Four paired images taken from a lens epithelial explant labeled with antibodies to CP49 (**A**–**D**) and α-tubulin (**A'**–**D'**). Red arrows in **A'**–**D'** mark sites where tubulin can be seen to be reduced or absent but are positive for CP49 (**A**–**D**; scale bar = 20 μm).

(white arrow) shows the immediate proximity of canonical 11 nm IFs at the periphery of the labeled structure. The change in shape resulting from the absence of these IFs suggests that those peripheral IFs exert control over the shape of this structure.

Figure 10 shows a montage of images taken from explants double-labeled with antibodies to CP49 (Figure 10A–D) and α-tubulin (Figure 10A'–D'). These data show a pattern similar to that observed for vimentin: α-tubulin appears to be largely excluded from the epithelial structure. Examples of the absence of α-tubulin that map exactly to the presence of CP49 are indicated with red arrows in Figure 10A'–D'.

Relationship to the aggresome: When cells are challenged by overexpression of a mutant protein that misfolds, a structure referred to as the aggresome can emerge [33-36]. The aggresome represents a site where ubiquitinated misfolded cytoplasmic proteins are concentrated by a microtubule-dependent process. Aggresomes appear to colocalize to the centrosome where they reside while autophagic processes are recruited to remove them [33]. Because the ultrastructure of this lens epithelial structure shows some similarity to some images generated for aggresomes, we conducted a colocalization of CP49 with markers for the aggresome: (a) γ-tubulin, a marker for the centrosome where aggresomes accumulate; (b) HDAC6, a bifunctional protein that links ubiquitinated

aggregated proteins to microtubules for transport to the centrosomal region to await autophagy [26,37,38]; and (c) ubiquitin, which is covalently linked to proteins targeted for degradation.

An epithelial explant double-labeled with antibodies to γ-tubulin (red channel) and CP49 (green channel) is shown in Figure 11. The data reveal examples of close proximity between the centrosome and the structure (e.g., red arrow) but also instances of no apparent relationship (e.g., yellow arrow), results that are consistent with the stochastic distribution of two perinuclear entities that are not physically linked.

Figure 12 shows the colocalization of CP49 (Figure 12A, green channel) and HDAC6 (Figure 12B, red channel) in a paraffin section that includes the epithelium. The merged image is seen in Figure 12C. Both proteins can be seen to localize to this structure, although the merged image suggests they do not map exactly.

Colocalization of CP49 (green channel) and ubiquitin (red channel) is shown in Figure 13. Although ubiquitin reactivity is scattered throughout the epithelium, ubiquitin shows no preferential localization to the CP49-rich vermiform structure.

DISCUSSION

CP49 and filensin are two of the most divergent members of the large family of cytoplasmic IF proteins [17,18]. Although expression of these two proteins is phylogenetically wide-spread [19], their expression has thus far been documented only in the lens fiber cell. Numerous reports have presented immunocytochemical and in situ hybridization data that are consistent with the conclusion that BF proteins are expressed in a robust manner after the commitment to fiber cell differentiation has been made. For these reasons, both proteins have been widely used as markers for fiber cell differentiation.

However, we report here that CP49 and filensin are found in the mouse lens epithelium, although only after 5 weeks of age. These data suggest that the mouse lens epithelial cell undergoes continued postnatal differentiation. For this reason, CP49 and filensin must also be considered markers of mouse lens epithelial cell differentiation.

To our knowledge, this is the first demonstration of such a late developmental change in the protein profile of the lens epithelium. Several mechanisms could account for the emergence of BF proteins in the epithelium at 5 weeks: the onset of transcription and translation at 5 weeks, constitutive
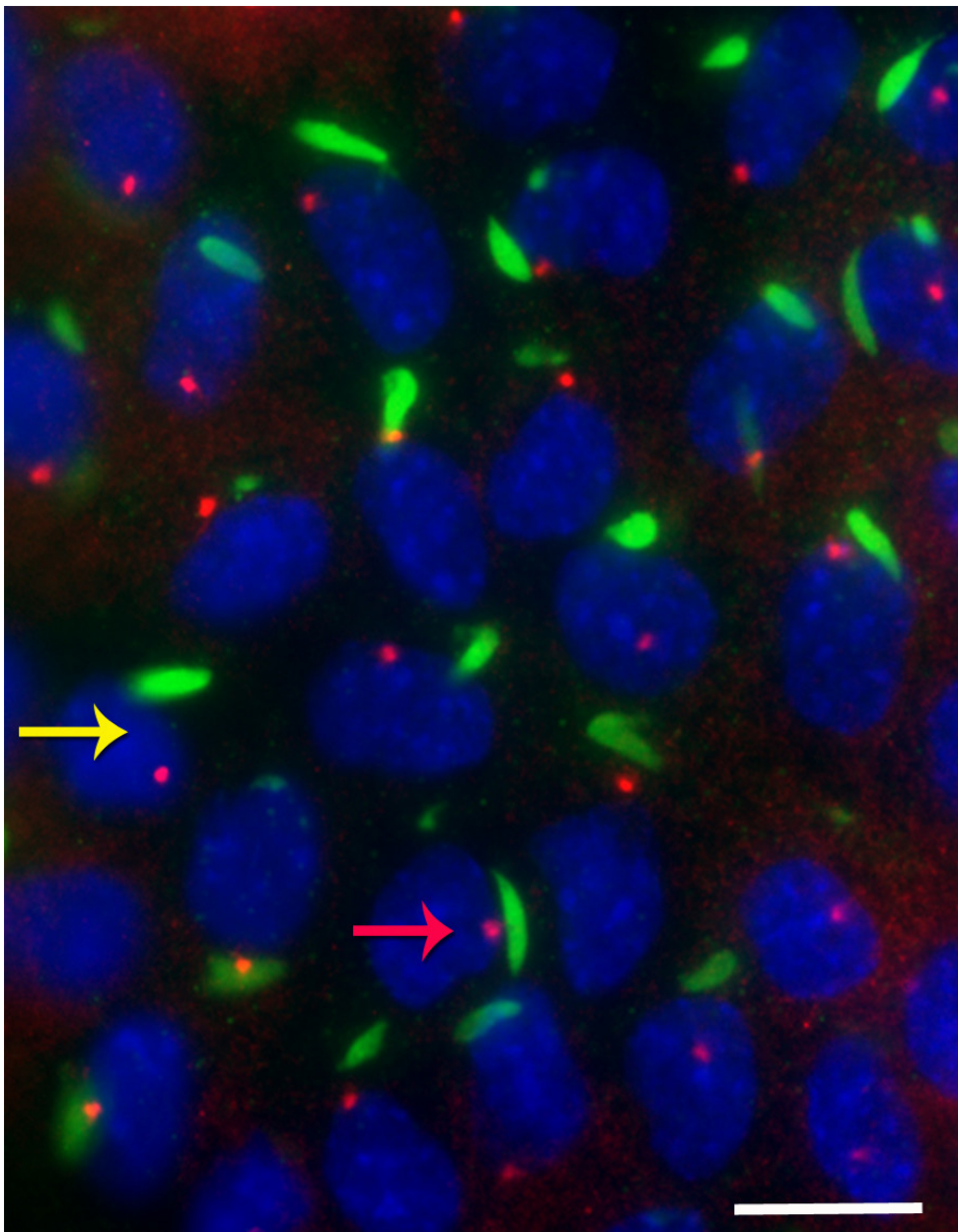

Figure 11. Co-localization of gamma tubulin and CP49. CP49 (green channel) and gamma tubulin (red channel) are co-localized in a lens epithelial explant. Yellow arrow marks a cell where the two signals are clearly unrelated, while the red arrow marks a cell where the signals are immediately adjacent.

transcription with the release of a translational block at 5 weeks, or constitutive transcription and translation, with a change in cytoplasmic conditions at 5 weeks that allowed the accumulation of BF proteins to commence. This change could be some stabilizing force, such as the onset of expression of a chaperone, or post-translational modifications. The contributions of these mechanisms is currently being explored. Data presented in a previous report [39] showed that in situ hybridization with probes for CP49 show high levels of CP49 transcripts in the embryonic fiber cell but no detectable evidence of transcripts in the epithelium, suggesting that CP49 transcription may not be constitutive in the lens epithelium.

Other reports have suggested that expression of at least one BF protein may occur in the lens epithelium. Ireland et al., using immunocytochemistry on embryonic human lenses, reported what appears to be transient expression of CP49 in the epithelium of the embryonic human lens in the 7- to 9-week-old age range [40], which subsequently disappears. Segev et al. [41] compared mRNA levels between the lens capsule and the epithelia acquired during cataract surgery from patients with senile cataract to that taken from

the postmortem lenses of individuals with clear lenses. The researchers reported that filensin is downregulated in tissues pooled from lenses diagnosed with senile cataract, suggesting that mRNA for filensin might be present in the adult human lens epithelium. However, given the abundance of filensin/CP49 mRNA in the underlying fiber cells, a small contamination of fiber cell material in just one of the samples used to generate the pooled epithelium for control studies could easily skew these results. If filensin were elevated while other fiber cell proteins were not, it would have ruled out such contamination. Further, although 9,700 human genes were represented on the chip used in these studies, it is not clear whether or which other fiber cell RNAs were present. Together, however, these reports open the door to the possibility that temporally-regulated expression of BF proteins in the lens epithelium may be a more phylogenetically widespread phenomenon.

Electron microscopy revealed that this structure is embedded in a meshwork of cytoskeletal filaments. Immunocytochemistry established that actin is highly enriched within this structure. The structure was first identified, in fact, by Rafferty's group in the 1980s, using fluorescent phalloidin, a probe for filamentous actin. Those studies revealed
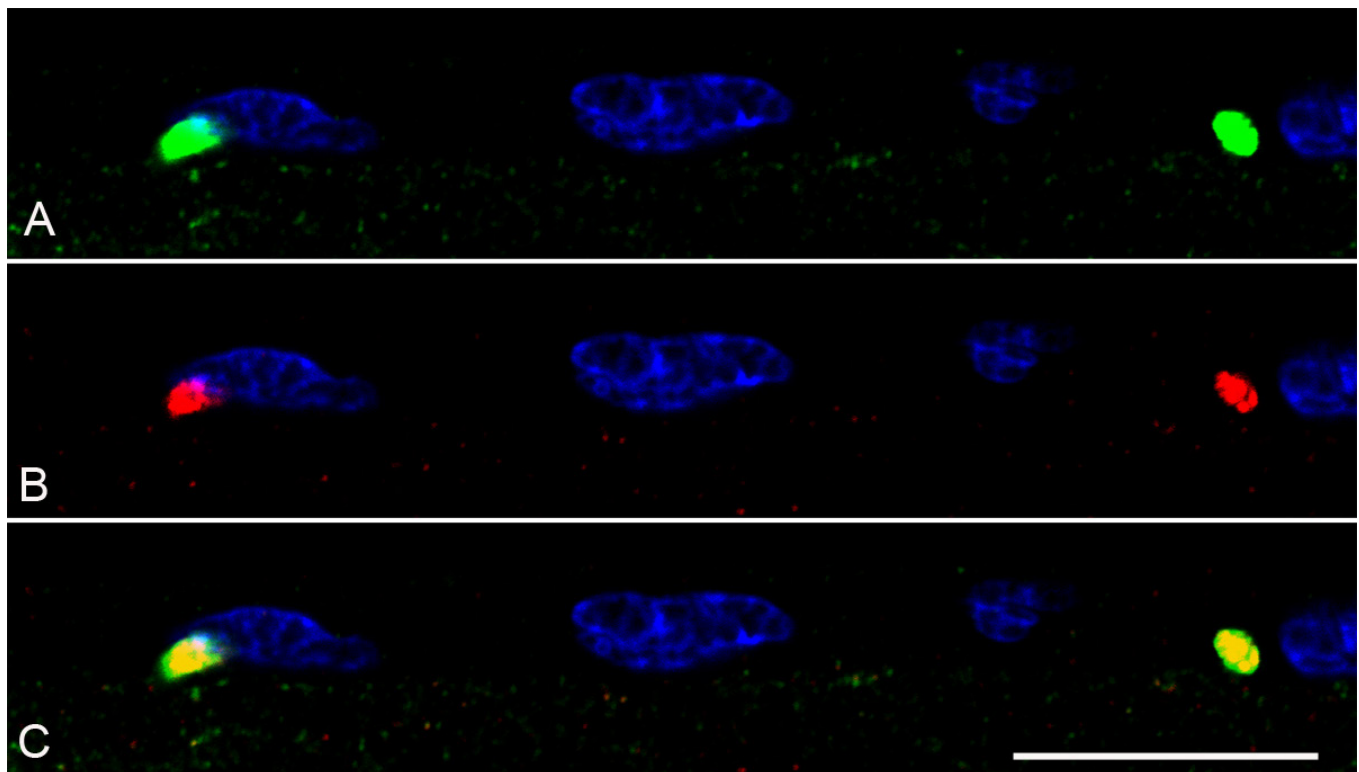

Figure 12. Colocalization of HDAC6 and CP49. High-magnification view of a small region of the mouse lens epithelium in a paraffin section. **A**: CP49 localization (green; 4',6-diamidino-2-phenylindole [DAPI] = blue). **B**: Histone deacetylase 6 (HDAC6) labeling. **C**: Merged. Scale bar = 10 μm.

the cortical actin network common to many cells but also described the vermiform structure as a sequestered actin bundle, or SAB [25]. At the time, the beaded filament story was still emerging; therefore, antibodies to BF proteins were not readily available. These investigators noted that the SAB was absent from some mice and concluded that it was a strain-specific phenomenon. In retrospect, this "strain-specificity" likely reflects the presence of a CP49 deletion mutation in some strains (e.g., FVB, 129svj) that results in the absence of the BF, and thus the absence of the vermiform structure [23,29,30]. These strains are commonly used in the generation of knockout and transgenic lines, which means that genetic manipulation of lenses in these strains usually produces a double knockout, or a transgenic line on a background of the CP49 knockout. The data presented here show that this structure will not assemble in the absence of the BF proteins; thus, actin is not sufficient for the assembly of this structure.

In contrast to actin, the IF protein vimentin and α-tubulin are largely excluded from this structure. Efforts to colocalize GFAP, another type III IF protein reported in the lenses of some strains of mice [31,32,42], showed that GFAP was not detectable in the lens epithelium of these mice, under the conditions used here. In the vimentin knockout, this structure forms, but it is more often round than vermiform. Thus, although vimentin is not required for assembly, this protein influences shape.

The data presented here also show a difference in the macromolecular organization of the BF proteins between fiber cells and epithelial cells. In the fiber cell, the BF is seen as a classic filamentous network that underlies the plasma membrane and spans the cytoplasm in a loosely arrayed meshwork [2,4,43,44], as shown in Figure 4E. In the epithelium, however, the BF is seen as a dense, well-delimited structure that does not underlie the plasma membrane or form a filamentous meshwork that spans the cell. The BF proteins in this condensed epithelial structure may actually be assembled into BFs, but this is not evident, possibly because of the compacted nature of the vermiform structure.

Electron microscopy of this epithelial structure showed some similarity to what has been described for the aggresome [33,35]. Aggresomes have been widely reported in cell culture systems transfected with mutant proteins known to misfold and subsequently accumulate, that is, experimental systems
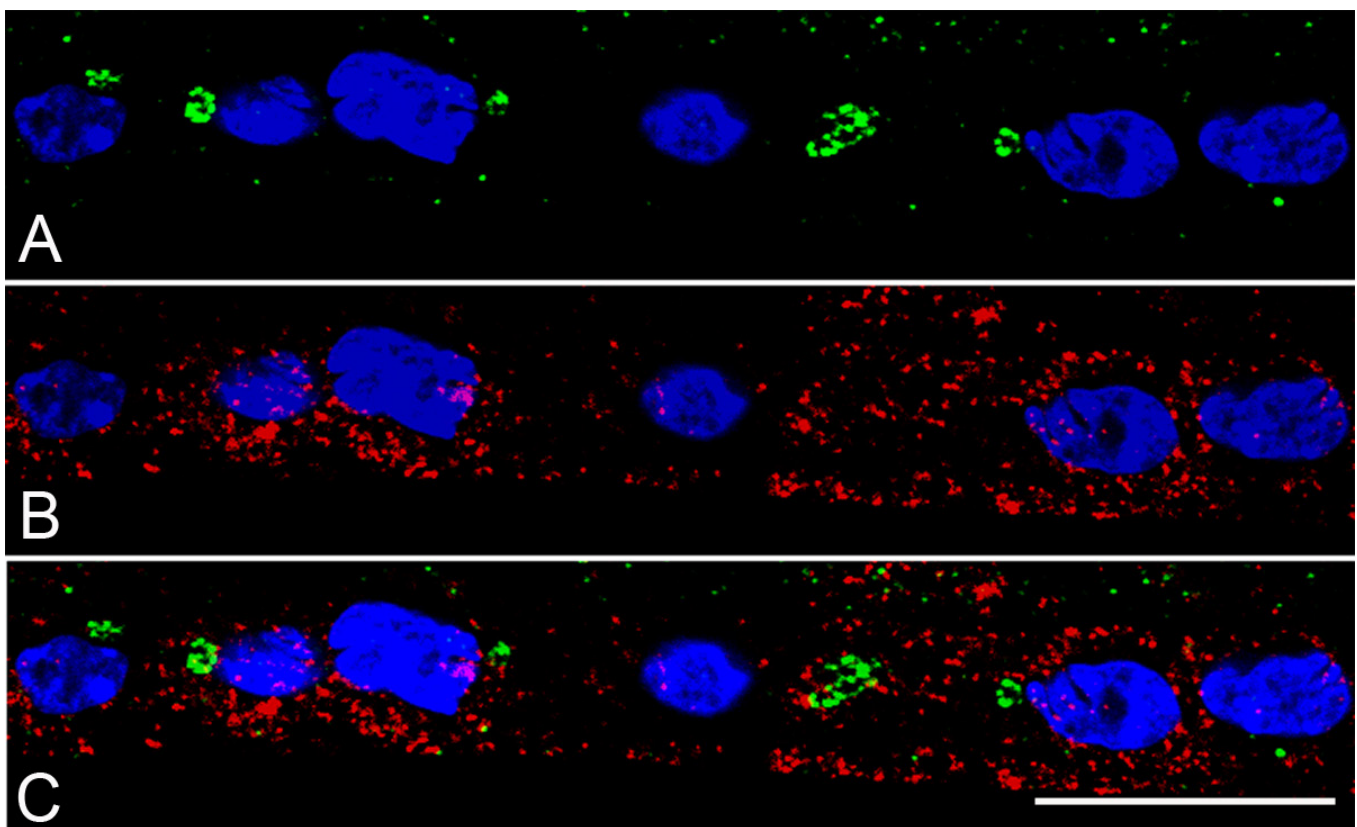

Figure 13. Co-localization of CP49 and Ubiquitin. Anterior lens epithelium showing the localization of CP49 (green channel) and ubiquitin (red channel). The lens is oriented with the anterior pole at 6:00. Scale bar = 10 μm.

with experimentally overdriven expression of misfolded proteins. Aggresomes have also been seen in pathologic conditions, such as in Huntington's disease [26,34,38,45,46]. In these systems, the misfolded protein is ubiquitinated, and then with the help of HDAC6 and the microtubule system, the aggregates are moved to and concentrated in the centrosomal region. Here, they coalesce into an aggresome that is ultimately removed by autophagy.

We have not found reports of large, stable aggresomes in normal WT tissues. The literature suggests that the long-term presence of aggresomes in a cell may be toxic and has been linked to increased apoptosis, double-stranded DNA breaks, cell-cycle arrest, and steric interference with the mitotic process [47]. The lens epithelial structure described here departs from of this description of the aggresome in several ways: (a) This structure is a stable presence in the lens epithelium of normal WT animals from 5 weeks to at least 1 year of age. (b) γ-tubulin, a spatial marker for the centrosome, does not show a preferential association with the vermiform structure. (c) Ubiquitin labeling is not preferentially concentrated in this structure. (d) Aggresomes appear to originate from numerous small particles that condense into less cohesive and ill-defined foci [46,48,49]. (e) The emergence of this structure is not stochastic as might be expected if misfolding were the structure's genesis. Instead, these structures appear in a temporally- and spatially-reproducible manner, and in a unique and uniformly shaped structure. The structure then appears to be dismantled in a similarly well-timed and programmed manner in the preequatorial zone, just before the onset of fiber cell differentiation. This "scheduled" dismantling suggests that the lens cell is equipped to remove this structure on some as yet unknown cue. (f) Finally, if this structure were serving as a repository for the misfolded BF protein, it would seem more likely to occur in the single knockout when only one of these insoluble proteins is expressed and where the insoluble assembly partner is left unmated. The opposite proved true: In the single knockout, where an unmated and insoluble protein might be expected to accumulate, the signal was absent. This behavior recapitulates what is seen in the fiber cells [3,20,21]. On the flip side, HDAC6, a marker for the aggresome, appears to be preferentially enriched in this structure, a feature that is consistent with what has been reported in aggresomes [26,37,38].

It is not clear what function is served by the expression of the BF proteins in the lens epithelium. The data presented here suggest that the BF proteins are not assembled into a classic cytoskeletal meshwork, either underlying the plasma membrane or spanning the cytoplasm. This would suggest

that the BF proteins in the epithelium do not serve the usual function of IF proteins in stabilizing the cellular phenotype.

The fact that these proteins do not emerge in the epithelium until about 5 weeks of age makes clear that BF proteins must now be considered markers of differentiation for epithelial and fiber cell differentiation in the mouse. Further, these data highlight a change in the protein profile of the mouse lens epithelium 5 weeks after birth. We are unaware of such a late emergence of any other protein in the lens epithelium. This suggests that differentiation of the lens epithelium continues well into the postnatal period.

Finally, the vermiform structure identified here shows some similarity to the aggresome, though many differences as well. If it is some variant of an aggresome, then, to our knowledge, it is the first demonstration of an aggresome that is uniformly expressed and stable in a healthy wild-type tissue. If this structure is unrelated to the aggresome, then the structure appears to be a novel organelle with, as yet, no known function.

REFERENCES

1. Maisel H, Perry MM. Electron microscope observations on some structural proteins of the chick lens. Exp Eye Res 1972; 14:7-12. [PMID: 4114289].

2. FitzGerald PG. Methods for the circumvention of problems associated with the study of the ocular lens plasma membrane-cytoskeleton complex. Curr Eye Res 1990; 9:1083-97. [PMID: 2095320].

3. Alizadeh A, Clark J, Seeberger T, Hess J, Blankenship T, FitzGerald PG. Targeted deletion of the lens fiber cell-specific intermediate filament protein filensin. Invest Ophthalmol Vis Sci 2003; 44:5252-8. [PMID: 14638724].

4. Yoon KH, Blankenship T, Shibata B, Fitzgerald PG. Resisting the effects of aging: a function for the fiber cell beaded filament. Invest Ophthalmol Vis Sci 2008; 49:1030-6. [PMID: 18326727].

5. Ireland M, Maisel H. A cytoskeletal protein unique to lens fiber cell differentiation. Exp Eye Res 1984; 38:637-45. [PMID: 6381079].

6. Ireland M, Maisel H. A family of lens fiber cell specific proteins. Lens Eye Toxic Res 1989; 6:623-38. [PMID: 2487275].

7. FitzGerald PG, Gottlieb W. The Mr 115 kd fiber cell-specific protein is a component of the lens cytoskeleton. Curr Eye Res 1989; 8:801-11. [PMID: 2791627].

8. Remington SG. Chicken filensin: a lens fiber cell protein that exhibits sequence similarity to intermediate filament proteins. J Cell Sci 1993; 105:1057-68. [PMID: 7693735].

9. Gounari F, Merdes A, Quinlan R, Hess J, FitzGerald PG, Ouzounis CA, Georgatos SD. Bovine filensin possesses

primary and secondary structure similarity to intermediate filament proteins. J Cell Biol 1993; 121:847-53. [PMID: 8491777].

10. Hess JF, Casselman JT, FitzGerald PG. cDNA analysis of the 49 kDa lens fiber cell cytoskeletal protein: a new, lens-specific member of the intermediate filament family? Curr Eye Res 1993; 12:77-88. [PMID: 7679620].

11. Hess JF, Casselman JT, FitzGerald PG. Gene structure and cDNA sequence identify the beaded filament protein CP49 as a highly divergent type I intermediate filament protein. J Biol Chem 1996; 271:6729-35. [PMID: 8636093].

12. Sawada K, Agata J, Eguchi G, Quinlan R, Maisel H. The predicted structure of chick lens CP49 and a variant thereof, CP49ins, the first vertebrate cytoplasmic intermediate filament protein with a lamin-like insertion in helix 1B. Curr Eye Res 1995; 14:545-53. [PMID: 7587300].

13. Hess JF, Casselman JT, Kong AP, FitzGerald PG. Primary sequence, secondary structure, gene structure, and assembly properties suggests that the lens-specific cytoskeletal protein filensin represents a novel class of intermediate filament protein. Exp Eye Res 1998; 66:625-44. [PMID: 9628810].

14. Carter JM, McLean WH, West S, Quinlan RA. Mapping of the human CP49 gene and identification of an intragenic polymorphic marker to allow genetic linkage analysis in autosomal dominant congenital cataract. Biochem Biophys Res Commun 2000; 270:432-6. [PMID: 10753642].

15. Masaki S, Quinlan RA. Gene structure and sequence comparisons of the eye lens specific protein, filensin, from rat and mouse: implications for protein classification and assembly. Gene 1997; 201:11-20. [PMID: 9409766].

16. Wallace P, Signer E, Paton IR, Burt D, Quinlan R. The chicken CP49 gene contains an extra exon compared to the human CP49 gene which identifies an important step in the evolution of the eye lens intermediate filament proteins. Gene 1998; 211:19-27. [PMID: 9573335].

17. Omary MB, Coulombe PA, McLean WH. Intermediate filament proteins and their associated diseases. N Engl J Med 2004; 351:2087-100. [PMID: 15537907].

18. Alberts B, ed. Molecular Biology of the Cell. 4th ed. New York: Garland Science; 2008.

19. FitzGerald PG, Casselman J. Immunologic conservation of the fiber cell beaded filament. Curr Eye Res 1991; 10:471-8. [PMID: 1889232].

20. Alizadeh A, Clark JI, Seeberger T, Hess J, Blankenship T, Spicer A, FitzGerald PG. Targeted genomic deletion of the lens-specific intermediate filament protein CP49. Invest Ophthalmol Vis Sci 2002; 43:3722-7. [PMID: 12454043].

21. Sandilands A, Prescott AR, Wegener A, Zoltoski RK, Hutcheson AM, Masaki S, Kuszak JR, Quinlan RA. Knockout of the intermediate filament protein CP49 destabilises the lens fibre cell cytoskeleton and decreases lens optical quality, but does not induce cataract. Exp Eye Res 2003; 76:385-91. [PMID: 12573667].

22. Fudge DS, McCuaig JV, Van Stralen S, Hess JF, Wang H, Mathias RT, FitzGerald PG. Intermediate filaments regulate tissue size and stiffness in the murine lens. Invest Ophthalmol Vis Sci 2011; 52:3860-7. [PMID: 21345981].

23. Alizadeh A, Clark J, Seeberger T, Hess J, Blankenship T, FitzGerald PG. Characterization of a mutation in the lens-specific CP49 in the 129 strain of mouse. Invest Ophthalmol Vis Sci 2004; 45:884-91. [PMID: 14985306].

24. Reichelt J, Bussow H, Grund C, Magin TM. Formation of a normal epidermis supported by increased stability of keratins 5 and 14 in keratin 10 null mice. Mol Biol Cell 2001; 12:1557-68. [PMID: 11408568].

25. Rafferty NS, Scholz DL. Actin in polygonal arrays of microfilaments and sequestered actin bundles (SABs) in lens epithelial cells of rabbits and mice. Curr Eye Res 1985; 4:713-8. [PMID: 4040842].

26. Gao YS, Hubbert CC, Lu J, Lee YS, Lee JY, Yao TP. Histone deacetylase 6 regulates growth factor-induced actin remodeling and endocytosis. Mol Cell Biol 2007; 27:8637-47. [PMID: 17938201].

27. Sun NS. B; Hess, J; FitzGerald, P. An alternative means of retaining ocular structure and improving immunoreactivity for light microscopy studies. Mol Vis 2015; In press.

28. Colucci-Guyon E, Portier MM, Dunia I, Paulin D, Pournin S, Babinet C. Mice lacking vimentin develop and reproduce without an obvious phenotype. Cell 1994; 79:679-94. [PMID: 7954832].

29. Sandilands A, Wang X, Hutcheson AM, James J, Prescott AR, Wegener A, Pekny M, Gong X, Quinlan RA. Bfsp2 mutation found in mouse 129 strains causes the loss of CP49' and induces vimentin-dependent changes in the lens fibre cell cytoskeleton. Exp Eye Res 2004; 78:875-89. [PMID: 15037121].

30. Simirskii VN, Lee RS, Wawrousek EF, Duncan MK. Inbred FVB/N mice are mutant at the cp49/Bfsp2 locus and lack beaded filament proteins in the lens. Invest Ophthalmol Vis Sci 2006; 47:4931-4. [PMID: 17065509].

31. Boyer S, Montagutelli X, Gomes D, Simon-Chazottes D, Guenet JL, Dupouey P. Recent evolutionary origin of the expression of the glial fibrillary acidic protein (GFAP) in lens epithelial cells. A molecular and genetic analysis of various mouse species. Brain Res Mol Brain Res 1991; 10:159-66. [PMID: 1712888].

32. Hatfield JS, Skoff RP, Maisel H, Eng L. Glial fibrillary acidic protein is localized in the lens epithelium. J Cell Biol 1984; 98:1895-8. [PMID: 6373785].

33. Johnston JA, Illing ME, Kopito RR. Cytoplasmic dynein/dynactin mediates the assembly of aggresomes. Cell Motil Cytoskeleton 2002; 53:26-38. [PMID: 12211113].

34. Johnston JA, Ward CL, Kopito RR. Aggresomes: a cellular response to misfolded proteins. J Cell Biol 1998; 143:1883-98. [PMID: 9864362].

35. Kopito RR. Aggresomes, inclusion bodies and protein aggregation. Trends Cell Biol 2000; 10:524-30. [PMID: 11121744].

36. Kopito RR, Sitia R. Aggresomes and Russell bodies. Symptoms of cellular indigestion? EMBO Rep 2000; 1:225-31. [PMID: 11256604].

37. Kawaguchi Y, Kovacs JJ, McLaurin A, Vance JM, Ito A, Yao TP. The deacetylase HDAC6 regulates aggresome formation and cell viability in response to misfolded protein stress. Cell 2003; 115:727-38. [PMID: 14675537].

38. Lee JY, Koga H, Kawaguchi Y, Tang W, Wong E, Gao YS, Pandey UB, Kaushik S, Tresse E, Lu J, Taylor JP, Cuervo AM, Yao TP. HDAC6 controls autophagosome maturation essential for ubiquitin-selective quality-control autophagy. EMBO J 2010; 29:969-80. [PMID: 20075865].

39. FitzGerald PG. Lens intermediate filaments. Exp Eye Res 2009; 88:165-72. [PMID: 19071112].

40. Ireland ME, Wallace P, Sandilands A, Poosch M, Kasper M, Graw J, Liu A, Maisel H, Prescott AR, Hutcheson AM, Goebel D, Quinlan RA. Up-regulation of novel intermediate filament proteins in primary fiber cells: an indicator of all vertebrate lens fiber differentiation? Anat Rec 2000; 258:25-33. [PMID: 10603445].

41. Segev F, Mor O, Segev A, Belkin M, Assia EI. Downregulation of gene expression in the ageing lens: a possible contributory factor in senile cataract. Eye (Lond) 2005; 19:80-5. [PMID: 15105821].

42. Hatfield JS, Skoff RP, Maisel H, Eng L, Bigner DD. The lens epithelium contains glial fibrillary acidic protein (GFAP). J Neuroimmunol 1985; 8:347-57. [PMID: 3891782].

43. Sandilands A, Prescott AR, Carter JM, Hutcheson AM, Quinlan RA, Richards J, FitzGerald PG. Vimentin and CP49/filensin form distinct networks in the lens which are independently modulated during lens fibre cell differentiation. J Cell Sci 1995; 108:1397-406. [PMID: 7615661].

44. Sandilands A, Prescott AR, Hutcheson AM, Quinlan RA, Casselman JT, FitzGerald PG. Filensin is proteolytically processed during lens fiber cell differentiation by multiple independent pathways. Eur J Cell Biol 1995; 67:238-53. [PMID: 7588880].

45. Bersuker K, Hipp MS, Calamini B, Morimoto RI, Kopito RR. Heat shock response activation exacerbates inclusion body formation in a cellular model of Huntington disease. J Biol Chem 2013; 288:23633-8. [PMID: 23839939].

46. Mukai H, Isagawa T, Goyama E, Tanaka S, Bence NF, Tamura A, Ono Y, Kopito RR. Formation of morphologically similar globular aggregates from diverse aggregation-prone proteins in mammalian cells. Proc Natl Acad Sci USA 2005; 102:10887-92. [PMID: 16040812].

47. Lu M, Boschetti C, Tunnacliffe A. Long Term Aggresome Accumulation Leads to DNA Damage, p53-dependent Cell Cycle Arrest, and Steric Interference in Mitosis. J Biol Chem 2015; 290:27986-8000. [PMID: 26408200].

48. Gilchrist CA, Gray DA, Stieber A, Gonatas NK, Kopito RR. Effect of ubiquitin expression on neuropathogenesis in a mouse model of familial amyotrophic lateral sclerosis. Neuropathol Appl Neurobiol 2005; 31:20-33. [PMID: 15634228].

49. Iwata A, Riley BE, Johnston JA, Kopito RR. HDAC6 and microtubules are required for autophagic degradation of aggregated huntingtin. J Biol Chem 2005; 280:40282-92. [PMID: 16192271].